Culture medium associated changes in the core proteome of macrophages and in their responses to copper oxide nanoparticles

Bastien Dalzon, Hélène Diemer, Véronique Collin-Faure, Sarah Cianférani, Thierry Rabilloud, Catherine Aude-Garcia

This manuscript has been published in Proteomics (2016) 16(22):2864-2877, under the doi: 10.1002/pmic.201600052

Culture medium-associated changes in the core proteome of macrophages and in their responses to copper oxide nanoparticles.

Bastien Dalzon [1,2,3] , Hélène Diemer [4,5] , Véronique Collin-Faure [1,2,3] , Sarah Cianférani [4,5], Thierry Rabilloud [1,2,3]* , Catherine Aude-Garcia[1,2,3]*

1: CEA Grenoble, BIG/CBM, Laboratory of Chemistry and Biology of Metals, Grenoble, France

2: Univ. Grenoble Alpes, Laboratory of Chemistry and Biology of Metals, Grenoble, France

3: CNRS UMR 5249, Laboratory of Chemistry and Biology of Metals, Grenoble, France

4: IPHC, Université de Strasbourg, BioOrganic Mass Spectrometry Laboratory (LSMBO), 25 rue Becquerel 67087 Strasbourg, France

5: CNRS UMR 7178, BioOrganic Mass spectrometry Laboratory (LSMBO), 25 rue Becquerel 67087 Strasbourg, France

*: to whom correspondence should be addressed:
Laboratoire de Chimie et Biologie des Métaux, UMR CNRS-CEA-UJF 5249, BIG/CBM, CEA Grenoble, 17 rue des martyrs, F-38054 Grenoble Cedex 9, France
thierry.rabilloud@cea.fr
catherine.aude-garcia@cea.fr

ABSTRACT

The physiology of cells cultured in vitro depends obviously on the external conditions, including the nutrients present in the culture medium. In order to test the influence of this parameter, J774 macrophages grown either in RPMI or in DMEM were compared by a combination of targeted analyses and a proteomic approach. The two media differ in their glucose, amino acids and vitamins concentrations, but there was no significant differences in the cell cycle nor in the percentage of phagocytic cells in both media, although the phagocytic capacity (i.e the number of phagocytized particles) was higher in DMEM. Conversely, we found that J774 cells grown in RPMI produced more NO in response to LPS. The proteomic study highlighted differences affecting the central metabolism and the nucleotide metabolism, the cytoskeleton, protein degradation and cell signaling. Furthermore, proteomics showed that J774 cells grown in RPMI or in DMEM and exposed to copper oxide nanoparticles respond rather differently, with only a few proteins similarly modulated between cells grown in both media. Taken together, our results show that the basal state of cells grown in two different media is different and this may affect the way they respond to an external stimulus or stress.

SIGNIFICANCE

The present study uses a combination of targeted and proteomics approaches to investigate an often-overlooked question, which is the dependance of cellular physiology on the composition of the culture medium. Although classical tests do not show strong differences, proteomics shows a number of differences in the core proteome, which reflect in the cell physiology. More importantly, the responses of cells grown in different media to a common stress are also appreciably different. By extension, these results suggest that the responses observed in vitro may be altered by subtle differences in the culture protocols, e.g. choice of starting medium, but also medium consumption induced by different inoculum concentrations and pretreatment time.

INTRODUCTION

Proteomic approaches have been used since the very dawn of the field to investigate cellular responses in vitro to various conditions, such as proliferation [1, 2], cell signaling [3-5], differentiation [6, 7] or cell resistance to antitumor drugs [8-10], just to quote a few papers in this area published before 2000. This area of research has considerably expanded over time, as shown by the hundreds of papers cited in a recent review about proteomics in toxicology [11].

All the papers in this subfield, however, are made on the same structure, i.e. comparing control cells to treated ones in a given medium, and this poses the problem of the influence of the medium itself on the state of the cells and thus on their responsiveness to stimuli. Culture media are optimized for both cell growth and convenience. For example, several classical media include rather high aminoacids and glucose concentration to let cells consume these nutrients without needing to refeed cell cultures every day. This rise the possibility that the nutrient concentrations may orient the metabolism of the cells and in turn their proteome, thereby altering their responses to the stimuli on interest.

This parameter is however quite difficult to investigate, because cells usually grow well in one culture medium and in limited variations of this "canonical" medium. Thus, if the influence of the culture medium is to be investigated, there are two caveats. In the first case, the different media are selected to keep the cells in similar states and usually the media differ very little, so that very limited changes can be expected. In the second, opposite case, the media are made very different, but then the cell growth is so altered in the suboptimal medium that the comparison makes little sense.

One happy exception to this situation is represented by some differentiated blood cell lines, such as the mouse plasmocyte or macrophage cell lines, which grow equally well in RPMI1640 and in DMEM media. These two media differ by a number of parameters [12]: the high-glucose DMEM medium contains twice more glucose than the RPMI medium, and is also richer in many amino acids (e.g. histidine, lysine, hydrophobic amino acids, and vitamins (e.g. folate, nicotinamide, pantothenate) and in some ions (e.g. calcium and magnesium). It also contains pyruvate, which RPMI does not. RPMI contains asparagine, aspartate and glutamate (not present in DMEM), is richer than DMEM in arginine, inositol and phosphate. The two media are therefore different enough to be expected to alter the physiology of the cells and thus their proteome. If the physiology of the same cell line becomes slightly different, it can then be expected that their responses to a stimulus may also be different.

In order to test these two levels of responses, i.e. the response intrinsic to the medium itself and the variations in the responses induced by the same stimulus in the two different media, we used the mouse macrophage cell line J774, grown in high glucose DMEM or in RPMI, and copper oxide nanoparticles as the stimulus, as we already have investigated the proteome changes induced by these particles in RPMI-grown J774 cells [13].

MATERIAL AND METHODS

Nanoparticles

Copper oxide (catalog number# 544868, from Sigma) was resuspended and coated with PVP 40 (purchased from Sigma) as previously described [14]. The

characterization of the nanoparticles and of their aggregates in culture medium has been described previously [13, 14]. We also verified previously that PVP alone had no effects on the cells [13].

Cell culture

The mouse macrophage cell line J774A1 was purchased from the European Cell Culture Collection (Salisbury, UK). The cells were cultured in DMEM (containing 1mM pyruvate) + 10% fetal bovine serum or in RPMI1640 + 10% fetal bovine serum. Cells were seeded every two days at 200,000 cells/ml and harvested at 1,000,000 cells per ml. For treatment with nanoparticles, the following scheme was used: cells were first seeded at 500,000 cells/ml in T175 flasks (50 ml per flask). They were exposed to nanoparticles on the following day and harvested after a further 24 hours in culture. Cell viability was measured by trypan blue exclusion.
Under these culture conditions, the LD20 for copper oxide nanoparticles was determined to be 10µg/ml, and this concentration was used in further experiments.
All experiments involving cells were carried out on independent biological triplicates.

Cell cycle

After harvesting, the cell pellet (from 2 ml of culture) was fixed by addition of 0.5 ml of cold (4°C) 70% ethanol and resuspension by pipetting. After fixation at room temperature for 30 minutes, 5 ml of PBS were added to the cell suspension, and the cells were collected by centrifugation. The cell pellet was then resuspended in 0.3 ml of PBS containing 0.01mg/ml RNAse A and 0.01mg/ml propidium iodide. The cells were incubated for 20 minutes at room temperature and then analyzed on a FACSCalibur instrument (Beckton Dickinson) operated with an excitation at 488 nm and an emission wavelength of 600 nm. The percentage of cells in the different phases of the cycle was then determined with the Cellquest software.

Phagocytosis activity measurement

The phagocytic activity was measured using fluorescent latex beads (1µm diameter, green labelled, catalog number L4655 from Sigma) and flow cytometry, essentially as described in [14, 15].

Mitochondrial transmembrane potential assessment

The mitochondrial transmembrane potential was assessed by Rhodamine 123 uptake at non-quenching concentrations, in order to obtain valid indications of the transmembrane potential [16] . Briefly, cells were treated with 40 nM Rhodamine 123 in complete culture medium for 30 minutes at 37 °C. Cells were then harvested, rinsed twice in PBS+0.1% glucose and analysed by flow cytometry on a FACSCalibur instrument (Beckton Dickinson), using 488 nm excitation and 515 nm emission filters.

NO production

The cells were grown to confluence in a 6 well plate. Then half of the wells were

treated with 30 or 100 ng/ml LPS (from salmonella), and arginine monohydrochloride was added to all the wells (5 mM final concentration) to give a high concentration of substrate for the nitric oxide synthases. After 18 hours of incubation, the cell culture medium was recovered, centrifuged at 10,000 g for 10 minutes to remove cells and debris, and the nitrite concentration in the supernatants was read at 540 nm after addition of an equal volume of Griess reagent and incubation at room temperature for 30 minutes.

Enzyme assays

The enzymes were assayed according to published procedures. Lactate and malate dehydrogenase were assayed by a coupled assay using Nitro blue tetrazolium as the final acceptor and phenazine methosulfate as a relay [17]. Biliverdin reductase was assayed directly for the NADPH-dependent conversion of biliverdin into bilirubin, followed at 450nm [18]. Pyruvate kinase was assayed by decrease of NADH at 340 nm in a lactate dehydrogenase-coupled assay [19]. Transladolase was assayed in a coupled assay [20].

The cell extracts for enzyme assays were prepared by lysing the cells for 20 minutes at 0°C in Hepes 20 mM pH 7.5, MgCl2 2 mM, KCl 50 mM, EGTA 1 mM, SB 3-14 0.15% w/v, followed by centrifugation at 15,000g for 15 minutes to clear the extract. The protein concentration was determined by a dye-binding assay.

F-Actin staining

This experiment was performed essentially as described previously [21] . Cells were cultured on coverslips placed in 6-well plates and exposed to NPs for 24h at 37°C. At the end of the exposure time, cells were washed twice for 5 min at 4°C in PBS, fixed in 4% paraformaldehyde for 30 min at room temperature. After two washes (5min/4°C in PBS), they were permeabilized in Triton X100 0.1% for 5 min at room temperature. After two more washes in PBS, 500 nM Phalloidin-Atto 550 (Sigma) was added to the cells and let for 20 min at room temperature in the dark. Coverslips-attached cells were washed, placed on microscope slides (Thermo Scientific) using a Vectashield mounting medium containing DAPI (Eurobio) and imaged using a Leica TCS SP2 SE confocal microscope. The images were processed using the Leica confocal software.

Proteomics

The 2D gel based proteomic experiments were carried out on independent biological triplicates for all comparisons, essentially as previously described [14, 21]. However, detailed material and methods are provided below.

Sample preparation

The cells were collected by scraping, and then washed three times in PBS. The cells were then washed once in TSE buffer (Tris-HCl 10 mM pH 7.5, sucrose 0.25M, EDTA 1 mM), and the volume of the cell pellet was estimated. The pellet was resuspended in its own volume of TSE buffer. Then 4 volumes (respective to the cell suspension just prepared) of concentrated lysis buffer (urea 8.75 M, thiourea 2.5 M, CHAPS 5% w/v, TCEP-HCl 6.25 mM, spermine base 12.5 mM) were added and the solution was let to extract at room temperature for 1 hour. The nucleic acids were

then pelleted by ultracentrifugation (270,000 g at room temperature for 1 h), and the protein concentration in the supernatant was determined by a dye-binding assay [22]. Carrier ampholytes (Pharmalytes pH 3-10) were added to a final concentration of 0.4% (w/v), and the samples were kept frozen at -20°C until use.

Isoelectric focusing

Home-made 160 mm long 4-8 linear pH gradient gels [23] were cast according to published procedures [24]. Four mm-wide strips were cut, and rehydrated overnight with the sample, diluted in a final volume of 0.6 ml of rehydration solution (7 M urea, 2 M thiourea, 4% CHAPS, 0.4% carrier ampholytes (Pharmalytes 3-10) and 100mM dithiodiethanol [25, 26].
The strips were then placed in a Multiphor plate (GE Healthcare), and IEF was carried out with the following electrical parameters: 100V for 1 hour, then 300V for 3 hours, then 1000V for 1 hour, then 3400 V up to 60-70 kVh. After IEF, the gels were equilibrated for 20 minutes in Tris 125mM, HCl 100mM, SDS 2.5%, glycerol 30% and urea 6 M [27] . They were then transferred on top of the SDS gels and sealed in place with 1% agarose dissolved in Tris 125mM, HCl 100mM, SDS 0.4% and 0.005% (w/v) bromophenol blue.

SDS electrophoresis and protein detection

Ten percent gels (160x200x1.5 mm) were used for protein separation. The Tris taurine buffer system [28] was used and operated at a ionic strength of 0.1 and a pH of 7.9. The final gel composition is thus Tris 180mM, HCl 100 mM, acrylamide 10% (w/v), bisacrylamide 0.27%. The upper electrode buffer is Tris 50 mM, Taurine 200 mM, SDS 0.1%. The lower electrode buffer is Tris 50 mM, glycine 200 mM, SDS 0.1%. The gels were run at 25V for 1hour, then 12.5W per gel until the dye front has reached the bottom of the gel. Detection was carried out by a tetrathionate silver staining [29] .

Image analysis

The gels were scanned after silver staining on a flatbed scanner (Epson perfection V750), using a 16 bits grayscale image acquisition. The gel images were then analyzed using the Delta 2D software (v 3.6). Spots that were never expressed above 100 ppm of the total spots were first filtered out. Then, significantly-varying spots were selected on the basis of their Student T-test p-value between the treated and the control groups. Spots showing a p-value lower than 0.05 were selected. In order to estimate the proportion of false positives, which is always a problem in multiple testing experiments, the Storey-Tibshirani approach was used [30].

Protein identification and mass spectrometry

For protein identification, either analytical gels loaded at 200 µg/gel and stained with tetrathionate silver staining or preparative gels loaded at 500 µg/gel and stained with a "derated" silver stain [31] were used.
The spots selected for identification were excised from silver-stained gels and destained with ferricyanide/thiosulfate on the same day as silver staining in order to improve the efficiency of the identification process [32][33] . In gel digestion was

performed with an automated protein digestion system, MassPrep Station (Waters, Milford, USA). The gel plugs were washed twice with 50 µL of 25 mM ammonium hydrogen carbonate (NH_4HCO_3) and 50 µL of acetonitrile. The cysteine residues were reduced by 50 µL of 10 mM dithiothreitol at 57°C and alkylated by 50 µL of 55 mM iodoacetamide. After dehydration with acetonitrile, the proteins were cleaved in gel with 10 µL of 12.5 ng/µL of modified porcine trypsin (Promega, Madison, WI, USA) in 25 mM NH_4HCO_3. The digestion was performed overnight at room temperature. The generated peptides were extracted with 30 µL of 60% acetonitrile in 0.1% formic acid. Acetonitrile was evaporated under vacuum before nanoLC-MS/MS analysis.

NanoLC-MS/MS analysis was performed using a nanoACQUITY Ultra-Performance-LC (Waters Corporation, Milford, USA) coupled to the Synapt^{TM} High Definition Mass Spectrometer^{TM} (Waters Corporation, Milford, USA). The system was fully controlled by MassLynx 4.1 SCN639 (Waters Corporation, Milford, USA).

The nanoLC system was composed of ACQUITY UPLC® CSH130 C18 column (250 mm x 75 µm with a 1.7 µm particle size, Waters Corporation, Milford, USA) and a Symmetry C18 precolumn (20 mm × 180 µm with a 5 µm particle size, Waters Corporation, Milford, USA). The solvent system consisted of 0.1% formic acid in water (solvent A) and 0.1% formic acid in acetonitrile (solvent B). 4 µL of sample were loaded into the enrichment column during 3 min at 5 µL/min with 99% of solvent A and 1% of solvent B. Elution of the peptides was performed at a flow rate of 300 nL/min with a 8-35% linear gradient of solvent B in 9 minutes.

The tandem mass spectrometer was equipped with a Z-spray ion source and a lock mass system. The capillary voltage was set at 2.8 kV and the cone voltage at 35 V. Mass calibration of the TOF was achieved using fragment ions from Glu-fibrino-peptide B on the [50;2000] m/z range. Online correction of this calibration was performed with Glu-fibrino-peptide B as the lock-mass. The ion $(M+2H)^{2+}$ at m/z 785.8426 was used to calibrate MS data and the fragment ion $(M+H)^{+}$ at m/z 684.3469 was used to calibrate MS/MS data during the analysis.

For tandem MS experiments, the system was operated with automatic switching between MS (0.5 s/scan on m/z range [150;1700]) and MS/MS modes (0.5 s/scan on m/z range [50;2000]). The two most abundant peptides (intensity threshold 20 counts/s), preferably doubly and triply charged ions, were selected on each MS spectrum for further isolation and CID fragmentation using collision energy profile. Fragmentation was performed using argon as the collision gas.

Mass data collected during analysis were processed and converted into .pkl files using ProteinLynx Global Server 2.3 (Waters Corporation, Milford, USA). Normal background subtraction type was used for both MS and MS/MS with 5% threshold and polynomial correction of order 5. Smoothing was performed on MS/MS spectra (Savitsky-Golay, 2 iterations, window of 3 channels). Deisotoping was applied for MS (medium desisotoping) and for MS/MS (fast deisotoping).

For protein identification, the MS/MS data were interpreted using a local Mascot server with MASCOT 2.4.1 algorithm (Matrix Science, London, UK) against UniProtKB/SwissProt (version 2014_11, 547,085 sequences). The research was carried out in all species. Spectra were searched with a mass tolerance of 15 ppm for MS and 0.05 Da for MS/MS data, allowing a maximum of one trypsin missed cleavage. Carbamidomethylation of cysteine residues and oxidation of methionine residues were specified as variable modifications. Protein identifications were validated with at least two peptides with Mascot ion score above 30.

RESULTS

In order to check that cells cultures in RPMI or DMEM were reasonably comparable, we first examined their growth characteristics. The fact that they gave the same culture yield (5-fold multiplication in the cell numbers in 48 hours of culture) was a first indication. We however investigated the cell cycle in more detail, and the results are shown in Figure 1. The proportion of cells in the various phases of the cycle (G1, S and G2/M) was not significantly different between cells cultured in RPMI or in DMEM. A minor increase in cells in the G2/M phase can be noted for cells growing in DMEM, at the expense of cells in the S phase. However, the consequence is unnoticable in terms of cells yield (cell counts are multiplied by 5 over 2 days in both media).
We then investigated the differentiated functions of the cells, i.e. their phagocytic capacity and their LPS-dependent NO production. As shown in Figure 2A, the NO production upon LPS stimulation was greater for cells cultured in RPMI than for cells cultured in DMEM, as described previously [34]. The effect was more pronounced for lower doses of LPS used as a stimulus, and as the concentration of tryptophan is 3 times higher in DMEM than in RPMI this was consistent with the proposed inhibition of NO production in DMEM through the stimulation of the aryl hydrocarbon receptor (AHR) by tryptophan-derived products [35]. This inhibition was however partially levied by higher doses of LPS, as shown in Figure 2A.

Regarding the phagocytic activity, the percentage of phagocytic cells is similar in both media, as shown on Figure 2B. However, the mean fluorescence (MRI, Figure 2C), which is an index of the average number of beads internalized by the cells, is 1.5 times higher in DMEM than in RPMI, showing that in this medium, the J774 cells are able to phagocytize more beads than in RPMI. These subtle differences in cellular functions suggested that the change in the culture medium may have a more global impact of the cells, which we investigated in more details via a 2D gel-based proteomic analysis.

The results, displayed in Figure 3 and Table 1, show that the gels were globally similar. Several significant differences were however found between cells grown in RPMI and cells grown in DMEM, affecting several cellular pathways, and the t-test distribution diagram (Supplementary Figure 1) suggested that most of these differences should be true positives.
Of course metabolic pathways were strongly represented (central metabolism, nucleotide metabolism and mitochondrion) but other functions or structural assemblies such as the cytoskeleton, the proteasome or proteins implied in cell signaling were also modulated from one culture medium to the other.
In order to validate some of these findings, we first assessed the mitochodondrial transmembrane potential. The results, displayed on figure 4, show that the average transmembrane potential is ca. 1.5 fold higher in DMEM than in RPMI, which is consistent with the greater richness in nutrients in DMEM.

We then measured some of the metabolic enzymes activities found through the proteomic screen, and the results are shown in Table 2. The activity measurements confirmed the proteomic-detected changes for malate dehydrogenase (+14% in DMEM), lactate dehydrogenase (+26% in DMEM) and pyruvate kinase (+32 % in

DMEM), while they did not for biliverdin reductase and transaldolase.
Finally, as many spots corresponding to cytoskeletal proteins involved in the actin cytoskeleton were found in the proteomic screen, we studied the actin cytoskeleton using labelled phalloidin and confocal microscopy. The results, displayed in Figure 5 and supplementary figure 2, show that cells grown in RPMI and DMEM have a different shape and different surface rugosity, as expected from changes in the actin cytoskeleton. Cells grown in RPMI are smaller and less adherent, with less ruffles but a lot of spiny plasma membrane extensions.

These medium-induced changes in the proteome led us to investigate whether besides the basal differences, the responses detected to a similar stimulus could be different for cells cultured in different media, on a proteomic scale. To this purpose, we treated J774 cells by copper oxide nanoparticles in DMEM, as we already had performed this study in RPMI [13]. In this context, it must be noted that we exposed the cells to the same concentration of nanoparticles (10µg/ml), corresponding to the LD20 in both media.
The proteomic results are shown for DMEM in Figure 6 and Table 3, which recapitulate both the results obtained in DMEM and those obtained in RPMI and published previously [13]. In both media 2200-2300 reproducible spots (i.e. present in all biological replicates) were analyzed, and the t-test distribution diagrams (supplementary figure 1) suggest that the proportion of false positives should be similarly low in both cases.

These results show that only a few proteins are similarly modulated by copper oxide nanoparticles in cells cultured in RPMI or in DMEM. These include the ferritin light chain, the regulatory subunit of glutamate cysteine ligase (GCLM), the HINT1 protein, the cGMP phosphodiesterase and the proteasome assembly chaperone. Others (e.g. mago-nashi) are even modulated in opposite directions by copper oxide in cells cultured in different media.

Finally, it shall be noted that more proteins are modulated in the case of the medium switch (74 protein species) than in response to copper oxide nanoparticles (43 proteins species in DMEM).

DISCUSSION

The above-detailed proteomic results can be analyzed at two levels. The first level concerns the physiological state in which the cells are in different culture media. As DMEM is twice richer than RPMI in glucose, in many amino acids and vitamins, changes in central metabolic enzymes are expected, and are indeed detected. However these changes are often of moderate amplitude (ca 20-30%) and are detected in a statistical filter because of the rather low data dispersion afforded by our proteomic setup.
It is noteworthy that although the glycolytic enzymes are very easily detected on 2D gels [36-38], we detected an increase in only the last enzyme of glycolysis (i.e. pyruvate kinase) and in two enzymes involved in the cytoplasmic reoxidation of NADH (i.e. lactate dehydrogenase and malate dehydrogenase) in cells grown in DMEM. This suggests a stronger Warburg effect in these cells, which is completely consistent with the high glucose content of DMEM.
It has also been recently described that glucose induced important changes in

macrophages, such as the glucose-driven reprogramming of macrophages [39], and the glucose-driven morphodynamics of macrophages [40], both observed on the closely related RAW264 macrophage cell line. In line with these observations, we observed changes in several proteins implicated in the actin cytoskeleton dynamics, and we confirmed important differences in the actin cytoskeleton between cells grown in RPMI and cells grown in DMEM. Culture medium-induced differences in the cell shape have previously been observed by Cohly et al., although they used a DMEM/F12 medium [34] instead of DMEM as we did. On a more functional point of view, these changes in the actin cytoskeleton are in line with the increase phagocytic capacity, as measured by the mean fluorescence of phagocytic cells (shown in Figure 2), in cells grown in DMEM.
In our case, the changes brought by the medium switch are however more complex than a simple change in glycolytic capacity, as the concentration of amino acids and vitamins also change. In this respect, aromatic amino acids are known to modulate the activity of the aromatic hydrocarbon receptor (AHR) [35], which induces an anti-inflammatory phenotype [41]. Thus, the medium change between RPMI and DMEM induces conflicting signals, high glucose driving a pro-inflammatory signal [42] and high tryptophan an anti-inflammatory signal. Under those precise circumstances, the anti-inflammatory signal overwhelms the pro-inflammatory signal from the medium, as shown in Figure 2. As expected, the level of inhibition decreases when the extraneous pro-inflammatory signal (i.e. the LPS concentration) increases.

In the same trend, several mitochondrial proteins and several proteins involved in nucleotide and nucleic acids metabolism are also modulated by the medium change. Here again, the changes are generally of moderate amplitude, and when stronger changes are observed (e.g. mcm7, pnph) they often concern only one minor protein form, the major one being almost unchanged.
This poses the question of the relevance of small changes that can even be restricted to one protein form and not to all of the various proteoforms of the same protein.
The various forms of the same protein detected in 2D gel spots most often correspond to charge variants induced by post translational modifications, e.g. phosphorylation or acetylation, and this has been used since the very early days of 2D electrophoresis (e.g. in [3]). However, the functional changes brought by post-translational modifications are not predictable a priori. For example, protein acetylation on lysines can either activate or deactivate proteins [43]. As another example, the RhoGDIs deactivate the Rho and Rac GTPases by sequestering them [44, 45]. However, modification of the RhoGDIs, e.g. by phosphorylation, removes them from the GTPases, which become active in turn [46, 47]. Thus, the activity of Rho and Rac, and the remodelling of the actin cytoskeleton in turn, does not correlate with the total amount of the RhoGDIs, but only with the amount of the modified RhoGDIs. This piece of data is easily accessible by 2D gel-based proteomics, but not by shotgun proteomics. The situation is however not always as simple, as shown by the example of transaldolase. Transaldolase has been shown to be regulated by post-translational modifications, but the spot pattern is very complex [48], so that there is no easy correlation between the overall activity and the precise abundance of some spots.
Overall, these various examples show that the final activity cannot be easily correlated with either the total amount of the protein or with the amount of a given spot. Our data both show the interest of the ability to deconvolute the various protein

forms and the necessity not to limit the protein identification scheme to the modulated spots, but also to their neighbors to pick out as many forms as possible of a given protein.

As different media obviously bring different states to the cells, they could also bring different levels of responses to external stimuli. While the responses to a physiological stimulus such as LPS have been shown to depend on the metabolic state of the cells [39], we also wanted to determine if this was the case for a toxic stimulus. Metallic nanoparticles represent one type of new, anthropic toxic stimulus to which macrophages are exposed, and we already have studied the proteomic response to copper oxide nanoparticles for both the RAW264 [14] and J774 [13] macrophages cell lines, both in the RPMI medium. We therefore carried out the same study on the same nanoparticles in the J774 cell line, but in the DMEM medium.
In such a comparative context, classical targeted biochemical studies only determine the level of responses (e.g. the level of NO produced in response to LPS). Proteomics can be seen as a highly parallel readout that produces quantitative responses for several hundreds of proteins at the same time. In addition, 2D gel-based proteomics also provide a view at changes at the protein species level, as shown by the Rho-GDIs examples. When examined in detail, the results obtained in comparative analyses (control cells vs nanoparticles-exposed cells in RPMI or DMEM) show different cases:

- for a few proteins (in our case the ferritin light chain, the GCLM and HINT1 proteins, the proteasome chaperone and cGMP phosphodiesterase, the changes are significant and in the same direction in both culture media. It is noteworthy that these changes are those with the highest amplitude (modulation factors of 2 and above), and affect primarily proteins known to be implied in responses to metallic stresses.

-for another few proteins, the changes are of the same amplitude in both media, and only the data dispersion explains why they are detected as significant in one medium and not in the other one. Examples include the formylglutathione hydrolase, Annexin A3, elongation factor Ts, the VPS 36 protein and the ferritin heavy chain. In the same trend, some proteins show a change of lesser amplitude in one medium compared to the other, leading to a change classified as significant in one case and not in the other (e.g. mitochondrial ribosomal protein L1, ERP29, MVB protein 4b, acylamino acid releasing enzyme, acidic form of the inositol polyphosphate phosphatase, GST omega 1, hippocalcin-like protein, coiled coil protein 51). Such cases are likely to occur in a process that is somewhat stochastic, as the proteomic analysis of complete cell extracts.

-for the majority of the modulated proteins, in most cases the modulation is present in one medium and absent in the other. In some extreme cases, however (e.g. the mago nashi protein and myosin 12B) the changes go in opposite directions in the two different media.

Nevertheless, when taken at the pathway level, the same pathways are altered when J774 cells respond to copper oxide nanoparticles in RPMI or in DMEM, with a very good consistency in response for the oxidative stress-related proteins. Conversely, mitochondrial proteins respond more to nanoparticles in DMEM than in RPMI, but

this may be linked to a different mitochondrial activity in the two media.

Finally, on a protein species point of view, it sometimes happens that one protein species is modulated in one culture medium and another protein species of the same protein in another medium (e.g. tropomodulin 3 and PCNA).

CONCLUDING REMARKS

The first lesson from this work is that a simple medium switch induces more changes in the core cellular proteome than responses to low toxicity nanoparticles such as titanium dioxide [13] or zinc dioxide [21]. Somewhat surprisingly, the classes of proteins modulated by the medium change go much beyond the metabolism-associated proteins in a wide sense (e.g. mitochondrial proteins and true metabolic enzymes). Structural proteins such as the cytoskeletal associated ones, as well as signaling-associated proteins are also modulated by the composition of the culture medium. Consequently, the cells are probably in a fairly different basal state depending on the culture medium, and it is therefore not surprising that they respond differently to the same stimulus in different culture media. Some core stress-related responses are however similar in the two different media, but the majority of the responses observed at the proteomic scale are different in the two different media. This further shows, if needed, how sensitive proteomic techniques are to the details of cellular physiology and metabolism. It also suggests that different responses reported in different studies on the same model may derive from subtle differences in the cell culture protocol, including of course the starting medium (as shown here) but probably extendable to the medium consumption, depending in turn on the cell inoculum and pretreatment time.

ACKNOWLEDGMENTS

This work was funded by the CNRS, The University of Grenoble, the University of Strasbourg Unistra, the Région Alsace, the Transverse Toxicology program of the CEA (Nanostress grant) and through the French National Agency for Research (ANR) (grant ANR-22 10-INBS-08; ProFI project, “Infrastructures Nationales en Biologie et Santé”; “Investissements d’Avenir” call). We thank the Fondation pour la Recherche Médicale for financial support of a Synapt HDMS mass spectrometer. BD also thanks the CNRS for a handicap PhD fellowship.

REFERENCES

[1] Bravo, R., Celis, J. E., A search for differential polypeptide synthesis throughout the cell cycle of HeLa cells. *J Cell Biol* 1980, *84*, 795-802.
[2] Bravo, R., Frank, R., Blundell, P. A., Macdonald-Bravo, H., Cyclin/PCNA is the auxiliary protein of DNA polymerase-delta. *Nature* 1987, *326*, 515-517.
[3] Chneiweiss, H., Beretta, L., Cordier, J., Boutterin, M. C.*, et al.*, Stathmin Is a Major Phosphoprotein and Cyclic Amp-Dependent Protein-Kinase Substrate in Mouse-Brain Neurons but Not in Astrocytes in Culture - Regulation During Ontogenesis. *Journal of Neurochemistry* 1989, *53*, 856-863.
[4] Doye, V., Boutterin, M. C., Sobel, A., Phosphorylation of Stathmin and Other Proteins Related to Nerve Growth Factor-Induced Regulation of Pc12 Cells. *Journal of Biological Chemistry* 1990, *265*, 11650-11655.
[5] Rasmussen, H. H., Celis, J. E., Evidence for an Altered Protein-Kinase-C (Pkc) Signaling Pathway in Psoriasis. *Journal of Investigative Dermatology* 1993, *101*, 560-566.
[6] Rabilloud, T., Berthier, R., Valette, C., Garin, J., Lawrence, L. J., Induction of Stathmin Expression During Erythropoietic Differentiation. *Cell Growth & Differentiation* 1995, *6*, 1307-1314.
[7] Rabilloud, T., Berthier, R., Vincon, M., Ferbus, D.*, et al.*, Early events in erythroid differentiation: Accumulation of the acidic peroxidoxin (PRP/TSA/NKEF-B). *Biochemical Journal* 1995, *312*, 699-705.
[8] Sinha, P., Hutter, G., Kottgen, E., Dietel, M.*, et al.*, Increased expression of annexin I and thioredoxin detected by two-dimensional gel electrophoresis of drug resistant human stomach cancer cells. *Journal of Biochemical and Biophysical Methods* 1998, *37*, 105-116.
[9] Sinha, P., Hutter, G., Kottgen, E., Dietel, M.*, et al.*, Search for novel proteins involved in the development of chemoresistance in colorectal cancer and fibrosarcoma cells in vitro using two-dimensional electrophoresis, mass spectrometry and microsequencing. *Electrophoresis* 1999, *20*, 2961-2969.
[10] Sinha, P., Hutter, G., Kottgen, E., Dietel, M.*, et al.*, Increased expression of epidermal fatty acid binding protein, cofilin, and 14-3-3-sigma (stratifin) detected by two-dimensional gel electrophoresis, mass spectrometry and microsequencing of drug-resistant human adenocarcinoma of the pancreas. *Electrophoresis* 1999, *20*, 2952-2960.
[11] Rabilloud, T., Lescuyer, P., Proteomics in mechanistic toxicology: history, concepts, achievements, caveats, and potential. *Proteomics* 2015, *15*, 1051-1074.
[12] Ham, R. G., McKeehan, W. L., Media and growth requirements. *Methods Enzymol* 1979, *58*, 44-93.
[13] Triboulet, S., Aude-Garcia, C., Armand, L., Collin-Faure, V.*, et al.*, Comparative proteomic analysis of the molecular responses of mouse macrophages to titanium dioxide and copper oxide nanoparticles unravels some toxic mechanisms for copper oxide nanoparticles in macrophages. *PLoS One* 2015, *10*, e0124496.
[14] Triboulet, S., Aude-Garcia, C., Carriere, M., Diemer, H.*, et al.*, Molecular responses of mouse macrophages to copper and copper oxide nanoparticles inferred from proteomic analyses. *Mol Cell Proteomics* 2013, *12*, 3108-3122.
[15] Abel, G., Szollosi, J., Fachet, J., Phagocytosis of fluorescent latex microbeads by peritoneal macrophages in different strains of mice: a flow cytometric study. *Eur J Immunogenet* 1991, *18*, 239-245.
[16] Perry, S. W., Norman, J. P., Barbieri, J., Brown, E. B., Gelbard, H. A.,

Mitochondrial membrane potential probes and the proton gradient: a practical usage guide. *Biotechniques* 2011, *50*, 98-115.
[17] Mayer, K. M., Arnold, F. H., A colorimetric assay to quantify dehydrogenase activity in crude cell lysates. *J Biomol Screen* 2002, *7*, 135-140.
[18] Baranano, D. E., Rao, M., Ferris, C. D., Snyder, S. H., Biliverdin reductase: a major physiologic cytoprotectant. *Proc Natl Acad Sci U S A* 2002, *99*, 16093-16098.
[19] Malcovati, M., Valentini, G., AMP- and fructose 1,6-bisphosphate-activated pyruvate kinases from Escherichia coli. *Methods Enzymol* 1982, *90 Pt E*, 170-179.
[20] Simcox, P. D., Reid, E. E., Canvin, D. T., Dennis, D. T., Enzymes of the Glycolytic and Pentose Phosphate Pathways in Proplastids from the Developing Endosperm of Ricinus communis L. *Plant Physiol* 1977, *59*, 1128-1132.
[21] Aude-Garcia, C., Dalzon, B., Ravanat, J. L., Collin-Faure, V.*, et al.*, A combined proteomic and targeted analysis unravels new toxic mechanisms for zinc oxide nanoparticles in macrophages. *J Proteomics* 2016, *134*, 174-185.
[22] Bradford, M. M., A rapid and sensitive method for the quantitation of microgram quantities of protein utilizing the principle of protein-dye binding. *Anal Biochem* 1976, *72*, 248-254.
[23] Gianazza, E., Celentano, F., Magenes, S., Ettori, C., Righetti, P. G., Formulations for immobilized pH gradients including pH extremes. *Electrophoresis* 1989, *10*, 806-808.
[24] Rabilloud, T., Valette, C., Lawrence, J. J., Sample application by in-gel rehydration improves the resolution of two-dimensional electrophoresis with immobilized pH gradients in the first dimension. *Electrophoresis* 1994, *15*, 1552-1558.
[25] Rabilloud, T., Adessi, C., Giraudel, A., Lunardi, J., Improvement of the solubilization of proteins in two-dimensional electrophoresis with immobilized pH gradients. *Electrophoresis* 1997, *18*, 307-316.
[26] Luche, S., Diemer, H., Tastet, C., Chevallet, M.*, et al.*, About thiol derivatization and resolution of basic proteins in two-dimensional electrophoresis. *Proteomics* 2004, *4*, 551-561.
[27] Gorg, A., Postel, W., Weser, J., Gunther, S.*, et al.*, Elimination of Point Streaking on Silver Stained Two-Dimensional Gels by Addition of Iodoacetamide to the Equilibration Buffer. *Electrophoresis* 1987, *8*, 122-124.
[28] Tastet, C., Lescuyer, P., Diemer, H., Luche, S.*, et al.*, A versatile electrophoresis system for the analysis of high- and low-molecular-weight proteins. *Electrophoresis* 2003, *24*, 1787-1794.
[29] Sinha, P., Poland, J., Schnolzer, M., Rabilloud, T., A new silver staining apparatus and procedure for matrix-assisted laser desorption/ionization-time of flight analysis of proteins after two-dimensional electrophoresis. *Proteomics* 2001, *1*, 835-840.
[30] Storey, J. D., Tibshirani, R., Statistical significance for genomewide studies. *Proc Natl Acad Sci U S A* 2003, *100*, 9440-9445.
[31] Morrissey, J. H., Silver stain for proteins in polyacrylamide gels: a modified procedure with enhanced uniform sensitivity. *Anal Biochem* 1981, *117*, 307-310.
[32] Gharahdaghi, F., Weinberg, C. R., Meagher, D. A., Imai, B. S., Mische, S. M., Mass spectrometric identification of proteins from silver-stained polyacrylamide gel: A method for the removal of silver ions to enhance sensitivity. *Electrophoresis* 1999, *20*, 601-605.
[33] Richert, S., Luche, S., Chevallet, M., Van Dorsselaer, A.*, et al.*, About the mechanism of interference of silver staining with peptide mass spectrometry.

Proteomics 2004, *4*, 909-916.
[34] Cohly, H., Stephens, J., Markhov, A., Angel, M.*, et al.*, Cell culture conditions affect LPS inducibility of the inflammatory mediators in J774A.1 murine macrophages. *Immunol Invest* 2001, *30*, 1-15.
[35] Heath-Pagliuso, S., Rogers, W. J., Tullis, K., Seidel, S. D.*, et al.*, Activation of the Ah receptor by tryptophan and tryptophan metabolites. *Biochemistry* 1998, *37*, 11508-11515.
[36] Petrak, J., Ivanek, R., Toman, O., Cmejla, R.*, et al.*, Deja vu in proteomics. A hit parade of repeatedly identified differentially expressed proteins. *Proteomics* 2008, *8*, 1744-1749.
[37] Wang, P., Bouwman, F. G., Mariman, E. C., Generally detected proteins in comparative proteomics--a matter of cellular stress response? *Proteomics* 2009, *9*, 2955-2966.
[38] Triboulet, S., Aude-Garcia, C., Armand, L., Gerdil, A.*, et al.*, Analysis of cellular responses of macrophages to zinc ions and zinc oxide nanoparticles: a combined targeted and proteomic approach. *Nanoscale* 2014, *6*, 6102-6114.
[39] Freemerman, A. J., Johnson, A. R., Sacks, G. N., Milner, J. J.*, et al.*, Metabolic reprogramming of macrophages: glucose transporter 1 (GLUT1)-mediated glucose metabolism drives a proinflammatory phenotype. *J Biol Chem* 2014, *289*, 7884-7896.
[40] Venter, G., Oerlemans, F. T., Wijers, M., Willemse, M.*, et al.*, Glucose controls morphodynamics of LPS-stimulated macrophages. *PLoS One* 2014, *9*, e96786.
[41] Esser, C., Rannug, A., The aryl hydrocarbon receptor in barrier organ physiology, immunology, and toxicology. *Pharmacol Rev* 2015, *67*, 259-279.
[42] Sharma, K., Danoff, T. M., DePiero, A., Ziyadeh, F. N., Enhanced expression of inducible nitric oxide synthase in murine macrophages and glomerular mesangial cells by elevated glucose levels: possible mediation via protein kinase C. *Biochem Biophys Res Commun* 1995, *207*, 80-88.
[43] Xiong, Y., Guan, K. L., Mechanistic insights into the regulation of metabolic enzymes by acetylation. *J Cell Biol* 2012, *198*, 155-164.
[44] Dovas, A., Couchman, J. R., RhoGDI: multiple functions in the regulation of Rho family GTPase activities. *Biochem J* 2005, *390*, 1-9.
[45] Garcia-Mata, R., Boulter, E., Burridge, K., The 'invisible hand': regulation of RHO GTPases by RHOGDIs. *Nat Rev Mol Cell Biol* 2011, *12*, 493-504.
[46] DerMardirossian, C., Rocklin, G., Seo, J. Y., Bokoch, G. M., Phosphorylation of RhoGDI by Src regulates Rho GTPase binding and cytosol-membrane cycling. *Mol Biol Cell* 2006, *17*, 4760-4768.
[47] DerMardirossian, C., Schnelzer, A., Bokoch, G. M., Phosphorylation of RhoGDI by Pak1 mediates dissociation of Rac GTPase. *Mol Cell* 2004, *15*, 117-127.
[48] Lachaise, F., Martin, G., Drougard, C., Perl, A.*, et al.*, Relationship between posttranslational modification of transaldolase and catalase deficiency in UV-sensitive repair-deficient xeroderma pigmentosum fibroblasts and SV40-transformed human cells. *Free Radic Biol Med* 2001, *30*, 1365-1373.

Table 1: Differentially-expressed proteins identified in the proteomic screen for cells grown in different media

Spot Ref.	Protein name	SwissProt acc. Nb.	predicted Mw (Da)	nb. pept.	seq. cov. (in %)	DMEM/RPMI fold/T-test
E1	Pyrroline carboxylate reductase	Q9DCC4	28720	5	18	1.20/0.04
E2	Aldose reductase	P45376	35732	5	15	1.27/0.01
E3	Malate dehydrogenase. cytosol.	P14152	36511	11	42	1.19/0.01
E4a	Lactate dehydrogenase	P06151	36499	4	13	1.33/0.04
E4b	Lactate dehydrogenase	P06151	36499	24	57	1.12/0.06
E5a	Transaldolase	Q93092	37387	8	26	0.73/0.01
E5b	Transaldolase	Q93092	37387	16	45	0.91/0.05
E5c	Transaldolase	Q93092	37387	17	46	1.03/0.90
E5d	Transaldolase	Q93092	37387	16	47	0.99/0.94
E6	Aldolase C	P05063	39395	10	23	1.14/0.04
E7a	Pyruvate kinase	P52480	57845	18	40	1.36/0.01
E7b	Pyruvate kinase	P52480	57845	24	57	0.90/0.01
E8	Asparagine synthetase	Q61024	64283	20	44	0.63/0.01
E9	Transketolase	P40142	67630	19	47	0.55/0.01
C1a	Cofilin 1	P18760	18560	2	17	1.99/0.01
C1b	Cofilin 1	P18760	18560	6	50	1.91/0.01
C2a	Rho gdi1	Q99PT1	23407	2	11	1.26/0.02
C2b	Rho gdi1	Q99PT1	23407	11	53	0.99/0.92
C3a	Rho gdi2	Q61599	22851	2	19	1.33/0.05
C3b	Rho gdi2	Q61599	22851	5	36	0.98/0.63
C4a	a-soluble NSF attach. Prot.	Q9DB05	33190	4	15	1.17/0.05
C4b	a-soluble NSF attach. Prot.	Q9DB05	33190	18	82	0.85/0.16
C5	Actin related protein 2	P61161	44761	16	45	0.84/0.01
C6	Tropomodulin 3	Q9JHJ0	39503	14	46	0.82/0.02
C7	Moesin	P26041	67767	27	47	0.75/0.02
C8	Vinculin	Q64727	116717	24	25	1.32/0.05
M1	ATP synthase subunit d. mitochondrial	Q9DCX2	18749	4	35	1.09/0.05
M2	Dihydrolipoyl acetyltransferase comp. PDH	Q8BMF4	67942	19	40	0.75/0.01
M3	2-oxoglutarate dehydrogenase. mito.	Q60597	116449	13	14	1.49/0.02
M4	Voltage-dependent anion channel 2	Q60930	31733	5	22	1.42/0.01
M5a	Glycine amidino transferase	Q9D964	48297	5	16	0.90/0.04
M5b	Glycine amidino transferase	Q9D964	48297	10	31	0.81/0.03
M6	NADH-ubiquin. oxidoreductase 75 kDa sub.	Q91VD9	79777	17	26	0.72/0.01
M7	MICOS complex subunit Mic60	Q8CAQ8	83900	31	46	0.67/0.03
M8	Lon protease. mitochondrial	Q8CGK3	105843	10	17	0.74/0.05

P1a	Translation initiation factor 5A-1	P63242	16832	4	21	1.44/0.01
P1b	Translation initiation factor 5A-1	P63242	16832	8	50	1.1/0.11
P2	Ribosomal protein rla0	P14869	34216	11	47	0.84/0.03
P3	Asparagine--tRNA ligase	Q8BP47	64279	6	35	0.62/0.03
P4	hsp90	P11499	83281	14	22	0.84/0.03
P5	Translation elongation factor 2	P58252	95314	45	60	0.80/0.01
Q1	Proteasome subunit beta6	Q60692	25379	10	69	1.22/0.02
Q2	Proteasome subunit beta2	Q9R1P3	22906	15	44	0.78/0.02
Q3	Proteasome regulatory subunit 8	Q9CX56	39930	7	18	1.26/0.01
Q4	Proteasome activator complex sub.1	P97371	28673	16	62	0.86/0.02
Q5	Ubiquitin carboxyl hydrolase L5	Q9WUP7	37617	17	71	0.76/0.05
Q6	SUMO activating enzyme 1	Q9R1T2	38620	2	71	0.55/0.01
Q7	Cathepsin D	P18242	44954	3	7	1.25/0.01
Q8	Serpin b6	Q60854	42599	8	23	0.83/0.03
S1	Inositol triphosphate pyrophosphatase	Q9D892	21897	7	60	1.19/0.02
S2	Acyl protein thioesterase 1	P97823	24688	6	42	1.34/0.01
S3	14-3-3 protein delta/zeta	P63101	27772	13	56	0.79/0.03
S4	14-3-3 protein gamma	P61982	28253	9	55	0.74/0.01
S5	EF hand domain protein 2	Q9D8Y0	26791	9	38	0.8/0.01
S6a	S/T kinase receptor associated protein	Q9Z1Z2	38443	16	34	1.17/0.01
S6b	S/T kinase receptor associated protein	Q9Z1Z2	38443	20	77	0.97/0.66
S7	MAP kinase 1	P63085	41278	20	67	0.80/0.02
S8	Protein phosphatase 1 reg. Subunit 7	Q3UM45	41294	16	47	1.12/0.05
S9	S/T-phosphatase 2A 55 kDa reg. Sub. Ba	Q6P1F6	51693	12	31	0.56/0.01
S10	Gnpi1	O88958	32550	8	29	1.59/0.01
N1	Pre-mRNA-splicing factor SPF27	Q9D287	26132	14	61	0.72/0.02
N2a	Purine nucleoside phosphorylase	P23492	32277	7	29	1.46/0.01
N2b	Purine nucleoside phosphorylase	P23492	32277	17	78	0.99/0.83
N3	Translin-associated protein X	Q9QZE7	32927	9	39	0.56/0.01
N4	DnaJ homolog subfamily C member 9	Q91WN1	30060	4	13	0.77/0.02
N5	Heterogeneous nuclear RNP C1/C2	Q9Z204	34385	12	35	0.63/0.03
N6	CCA tRNA nucleotidyltransferase 1. mito.	Q8K1J6	49897	6	16	0.53/0.01
N7	Adenosine kinase	P55264	40150	3	10	1.28/0.02
N8	Spliceosome RNA helicase Ddx39b	Q9Z1N5	49035	19	50	0.82/0.03
N9	Inosine monophosphate dehydrogenase 2	P24547	55817	26	57	0.75/0.01
N10	Heterogeneous nuclear ribonucleoprotein L	Q8R081	63964	5	9	1.21/0.03
N11	Far upstream element-binding protein 2	Q3U0V1	76775	2	3	1.34/0.01
N12a	DNA replication licensing factor MCM7	Q61881	81212	15	27	2.09/0.01
N12b	DNA replication licensing factor MCM7	Q61881	81212	27	46	0.92/0.46
N13	phosphoribosylformylglycinamidine synthase	Q5SUR0	144629	15	17	1.31/0.02

H1	Flavin/biliverdin reductase	Q923D2	22197	13	82	0.88/0.04
H2a	Biliverdin reductase A	Q9CY64	33525	10	35	0.71/0.01
H2b	Biliverdin reductase A	Q9CY64	33525	13	54	0.95/0.59
U1	Cytochrome b5a	P56395	15241	5	50	1.86/0.04
U2	Chloride intracellular channel protein 4	Q9QYB1	28731	15	71	0.83/0.01
U3	Delta-aminolevulinic acid dehydratase	P10518	36024	12	38	0.81/0.03
U4	Pyridoxal kinase	Q8K183	35014	9	38	0.74/0.04
U5	Annexin A3	O35639	36386	21	59	0.89/0.01
U6	Aldose reductase-related protein 2	P45377	36121	6	25	0.80/0.02
U7	Adenosylhomocysteinase	P50247	47689	17	50	0.71/0.01
U8	EH domain-containing protein 1	Q9WVK4	60605	29	55	0.41/0.01
U9	Bifunctional pA-phosphosulfate synthase 1	Q60967	70794	13	25	0.53/0.03
U10	von Willebrand A domain- protein 5A	Q99KC8	87145	19	25	0.81/0.01
U11	Insulin-degrading enzyme	Q9JHR7	117778	13	14	0.75/0.02

Table 2 : enzyme activities in J774 cells grown in RPMI or DMEM media

Enzyme	activity in RPMI-cultured cells	activity in DMEM-cultured cells	activity ratio DMEM/RPMI	T test DMEM vs RPMI
LDH	216.37 ± 11.59	272.50 ± 11.19	1.26	0.00043
MDH	56.87 ± 2.25	65.00 ±4.81	1.14	0.035
Transaldolase	30.31 ± 1.92	30.69 ± 1.25	1.01	0.756
Pyruvate kinase	190.48 ± 21.65	251.99 ± 19.97	1.32	0.0059
Billiverbin reductase	3.84 ± 1.02	3.87 ± 1.06	1.01	0.964

The units are expressed in µmole substrate converted /min/mg total protein.
The measures were made on four independent biological replicates

Table 3: Differentially-expressed proteins identified in the proteomic screen for cells exposed to copper oxide nanoparticles

Spot Number	protein name	Swissprot Acc. N°	predicted Mw	nb unique peptides	seq coverage	CuO/ctrl fold/T-test DMEM	CuO/ctrl fold/T-test RPMI
Metabolim							
E1	**Transaldolase**	**Q93092**	**37389**	**13**	**34%**	**1.23/0.01**	**1.04/0.80**
E2	*Aldose reductase*	*P45376*	*35732*	*20*	*60%*	*1.03/0.68*	*0.53/0.02*
E3	*Galactokinase*	*Q9R0N0*	*42295*	*3*	*8%*	*0.93/0.62*	*0.32/0.001*
Mitochondria							
M1	**Prohibitin**	**P67778**	**29821**	**19**	**85%**	**0.83/0.01**	**0.96/0.43**
M2	**Elongation factor Ts, mitochondrial**	**Q9CZR8**	**35334**	**2**	**12%**	**0.84/0.01**	**0.86/0.67**
M3	**Stomatin-like protein 2, mitochondrial**	**Q99JB2**	**38385**	**2**	**9%**	**0.50/0.05**	**0.95/0.86**
M4	**Hydroxymethylglutaryl-CoA lyase**	**P38060**	**34238**	**2**	**11%**	**0.7/0.01**	**1.42/0.20**
M5	**Persulfide dioxygenase ETHE1**	**Q9DCM0**	**27739**	**2**	**11%**	**0.65/0.04**	**1.14/0.25**
M6a	**ETFA**	**Q99LC5**	**35080**	**3**	**11%**	**0.58/0.03**	**1.38/0.10**
M6b	ETFA	Q99LC5	35080	4	16%	0.92/0.54	0.74/0.08
M7	**39S ribosomal protein L1, mitochondrial**	**Q99N96**	**37598**	**4**	**13%**	**0.77/0.01**	**0.88/0.55**
Cytoskeleton and trafficking							
C1	***Myosin regulatory light chain 12B***	***Q3THE2***	***19795***	***4***	***23%***	***2.0/0.02***	***0.54/0.01***
C2	**Dynactin subunit 3**	**Q9Z0Y1**	**20979**	**3**	**15%**	**1.40/0.03**	**0.70/0.28**
C3	**Septin-2**	**P42208**	**41526**	**9**	**35%**	**1.58/0.02**	**0.74/0.06**
C4a	**Rho GDP-dissociation inhibitor 2**	**Q61599**	**22852**	**2**	**19%**	**1.48/0.01**	**1.11/0.36**
C4b	Rho GDP-dissociation inhibitor 2	Q61599	22852	5	36%	1.01/0.82	0.98/0.68
C5	**Alpha-soluble NSF attachment protein**	**Q9DB05**	**33191**	**15**	**70%**	**1.26/0.01**	**0.96/0.83**
C6	**Endoplasmic reticulum protein 29**	**P57759**	**28825**	**3**	**13%**	**0.67/0.03**	**0.80/0.35**
C7	**VPS 36**	**Q91XD6**	**43737**	**2**	**6%**	**1.37/0.03**	**1.48/0.13**
C8a	*MAPREB1 (acidic spot)*	*Q61166*	*30016*	*3*	*17%*	*0.99/0.98*	*0.3/0.001*
C8b	*MAPREB1 (basic spot)*	*Q61166*	*30016*	*4*	*16%*	*1.11/0.22*	*0.7/0.04*
C9	*Charged MVB protein 4b*	*Q9D8B3*	*24936*	*4*	*17%*	*0.89/0.34*	*0.7/0.04*
C10a	*Tropomodulin-3*	*Q9JHJ0*	*39503*	*3*	*10%*	*1.16/0.28*	*0.54/0.025*
C10b	**Tropomodulin-3**	**Q9JHJ0**	**39503**	**14**	**46%**	**1.30/0.01**	**0.82/0.31**
C11	*Stathmin*	*P54227*	*17274*	*6*	*39%*	*0.94/0.50*	*0.49/0.04*
C12	*ARP 2/3 complex subunit 5*	*Q9CPW4*	*16288*	*4*	*27%*	*1.12/0.48*	*0.22/0.001*
Nucleic acids							
N1	5'(3')-deoxyribonucleotidase,	Q9JM14	23077	7	50%	1.23/0.05	0.69/0.07
N2	***Histidine triad nucleotide-binding protein 1***	***P70349***	***13777***	***8***	***79%***	***1.26/0.05***	***2.91/0.01***
N3	**Ribonuclease inhibitor**	**Q91VI7**	**49818**	**2**	**4%**	**1.72/0.01**	**0.78/0.61**
N4	***Protein mago nashi***	***P61327***	***17309***	***2***	***21%***	***0.49/0.04***	***2.62/0.03***

	homolog						
Protein production							
P1	**Protein disulfide-isomerase**	**P09103**	**57061**	**29**	**59%**	**1.15/0.03**	**0.92/0.24**
P2	**Acylamino-acid-releasing enzyme**	**Q8R146**	**81581**	**4**	**7%**	**1.24/0.02**	**1.11/0.80**
P3	**Threonine--tRNA ligase, cytoplasmic**	**Q9D0R2**	**83358**	**7**	**10%**	**0.62/0.01**	**0.96/0.80**
P4	*eIF3j*	*Q66JS6*	*29486*	*2*	*10%*	*1.67/0.21*	*0.46/0.025*
P5	*Elongation factor 1-delta*	*P57776*	*31293*	*2*	*13%*	*1.19/0.20*	*0.7/0.04*
Protein degradation							
Q1	**Proteasome activator complex subunit 2**	**P97372**	**27058**	**16**	**72%**	**1.58/0.03**	**0.89/0.23**
Q2	**Proteasome subunit alpha type-1**	**Q9R1P4**	**29547**	**17**	**83%**	**1.60/0.02**	**1.00/0.98**
Q3	***Proteasome assembly chaperone 4***	***P0C7N9***	***13974***	***4***	***42%***	***2.15/0.02***	***10.77/0.02***
Q4	**COMM domain-containing protein 4**	**Q9CQ02**	**21765**	**2**	**10%**	**1.54/0.01**	**0.76/0.18**
Q5	*Proteasome subunit beta type-9*	*P28076*	*23397*	*2*	*10%*	*1.08/0.60*	*0.45/0.01*
Q6	*Ubiquitin C-terminal hydrolase L3*	*Q9JKB1*	*26152*	*2*	*10%*	*1.24/0.31*	*0.42/0.02*
Signalling							
S1a	**Inositol polyphosphate 1-phosphatase**	**P49442**	**43348**	**3**	**7%**	**0.22/0.01**	**0.75/0.56**
S1b	Inositol polyphosphate 1-phosphatase	P49442	43348	3	9%	1.13/0.52	0.49/0.09
S2	***cGMP 3',5'-phosphodiesterase delta***	***O55057***	***17390***	***2***	***21%***	***1.86/0.01***	***2.19/0.02***
S3	**Dual specificity MAP kinase kinase 1**	**P31938**	**43440**	**3**	**7%**	**1.52/0.01**	**0.99/0.99**
S4	**Neudesin**	**Q9CQ45**	**18905**	**2**	**12%**	**1.48/0.03**	**0.75/0.09**
S5	**S/T phosphatase PP1-g catalytic subunit**	**P63087**	**36957**	**4**	**14%**	**0.46/0.03**	**1.21/0.54**
S6	*Inositol monophosphatase 1*	*O55023*	*30436*	*4*	*17%*	*0.97/0.93*	*0.65/0.045*
S7	*Guanine nucleotide-binding protein G*	*P08752*	*40489*	*4*	*13%*	*0.92/0.30*	*0.6/0.03*
Oxidative stress response							
H1	**Ferritin heavy chain**	**P09528**	**21067**	**3**	**17%**	**2.35/0.01**	**1.76/0.35**
H2	***Glutamate--cysteine ligase reg. subunit***	***O09172***	***30535***	***6***	***30%***	***1.85/0.01***	***1.735/0.02***
H3	***Ferritin light chain 1***	***P29391***	***20803***	***4***	***27%***	***1.97/0.01***	***1.65/0.03***
H4	**S-formylglutathione hydrolase**	**Q9R0P3**	**31320**	**6**	**38%**	**1.17/0.03**	**1.18/0.13**
H5	***Heme oxygenase 1***	***P14901***	***32911***	***5***	***25%***	***14.7/0.04***	***6.37/0.05***
H6	**Flavin/biliverdin reductase**	**Q923D2**	**22197**	**13**	**82%**	**1.34/0.01**	**0.98/0.93**
H7	*GSTomega-1*	*O09131*	*27498*	*4*	*18*	*0.84/0.33*	*0.53/0.01*
H8	*Peroxiredoxin-6*	*O08709*	*24871*	*6*	*33*	*1.12/0.40*	*0.83/0.01*
Unclassified							
U1	**Hippocalcin-like protein 1**	**P62748**	**22339**	**7**	**34%**	**1.50/0.01**	**1.24/0.17**
U2	*Pycard*	*Q9EPB4*	*21459*	*6*	*43%*	*1.03/0.69*	*0.51/0.04*
U3	**Annexin A3**	**O35639**	**36386**	**23**	**72%**	**0.76/0.01**	**0.73/0.08**
U4	**Coiled-coil domain-containing protein 51**	**Q3URS9**	**45133**	**6**	**17%**	**0.64/0.02**	**0.89/0.07**
U5	**Ufm1-specific**	**Q99K23**	**52516**	**2**	**6%**	**1.66/0.01**	**0.72/0.14**

	protease 2						
U6a	**Proliferating cell nuclear antigen**	**P17918**	**28786**	**13**	**66%**	**1.23/0.01**	**0.88/0.01**
U6b	*Proliferating cell nuclear antigen*	*P17918*	28786	*8*	*33*	*0.72/0.48*	*1.67/0.045*
U7	*Sepiapterin reductase*	*Q64105*	*27883*	*3*	*15*	*1.21/0.28*	*0.76/0.04*
U8	*Tumor protein D52*	*Q62393*	*24313*	*3*	*17*	*1.15/0.28*	*0.38/0.001*
U9	**NADPH oxidase p40**	**P97369**	**37389**	**16**	**44%**	**0.68/0.05**	**1.02/0.87**

Bold : statistically-differently expressed protein species for cells grown in DMEM and treated with copper oxide nanoparticles
Italics : statistically-differently expressed protein species for cells grown in RMPI and treated with copper oxide nanoparticles [17]
Bold italics : protein species common to both responses
Plain font : control protein species

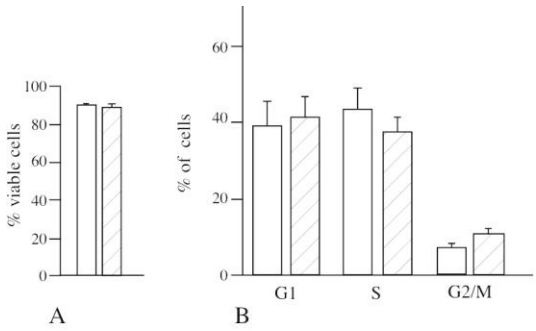

Figure 1: cell viability and cell cycle

In panel A, the viability of the cells cultured in RPMI (white bars) or DMEM (hatched bars) is indicated, showing no difference in cell death in both media. In panel B, the proportion of the cells in the three phases of the cell cycle is indicated. White bars, cells growing in RMPI, hatched bars, cells growing in DMEM.

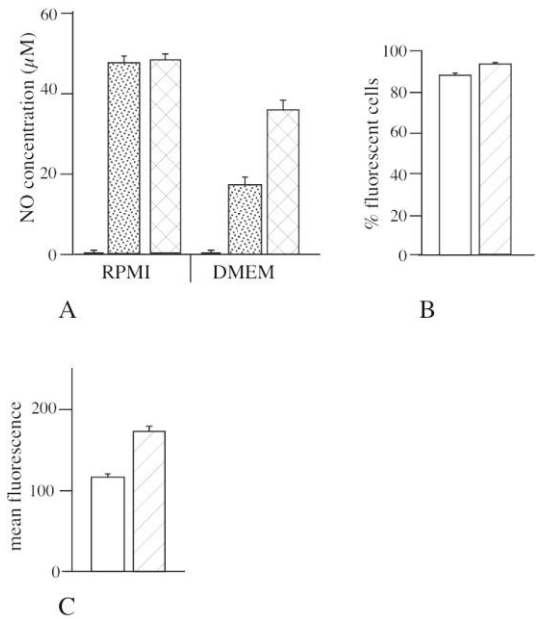

Figure 2: NO production in response to LPS and phagocytosis
In panel A, the NO production after LPS stimulation for 24 hours is described. Black bars: no LPS stimulation. Dotted bars: stimulation with 30 ng/ml LPS. Crossed bars: stimulation with 100 ng/ml LPS
In panel B, the proportion of phagocytic cells (i.e. cells able to ingest at least one bead in 2 hours is indicated. White bars: cells grown in RMPI. Hatched bars: cells grown in DMEM.
In panel C, the mean fluorescence index (MFI, i.e. the average fluorescence for the cells having ingested one or more beads) is indicated. White bars: cells grown in RMPI. Hatched bars: cells grown in DMEM.

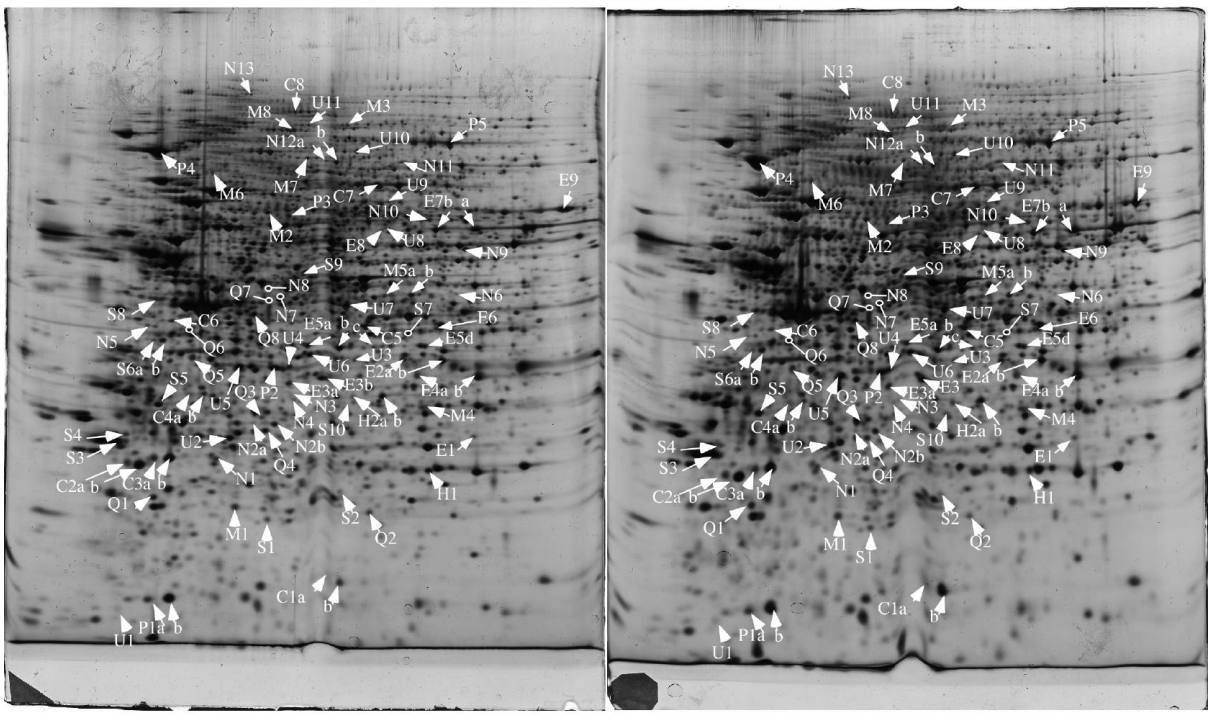

Figure 3: Proteomic analysis of total cell extracts by 2D electrophoresis: effect of culture medium

Total cell extracts of J774A1 cells were separated by two-dimensional gel electrophoresis.
The first dimensions covered a 4-8 pH range and the second dimension a 15-200 kDa range.
Total cellular proteins (150 µg) were loaded on the first dimension gel.

A: gel obtained from cells grown in RPMI
B: gel obtained from cells grown in DMEM

The arrows point to spots that show reproducible and statistically significant changes between the control and nanoparticles-treated cells and to the control neighbor spots in some cases. Spot numbering according to Table 1

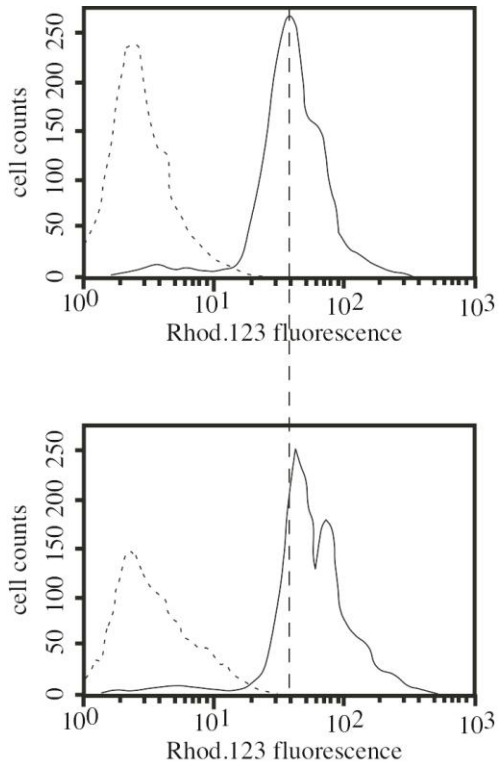

Figure 4: Study of the mitochondrial transmembrane potential

Top panel: Distribution of rhodamine 123 fluorescence for cells grown in RPMI. Dotted line: negative control (no rhodamine). Solid line: positive control (40nM rhodamine 123, 30 minutes). The mean fluorescence is 2.5±0.1 units for the negative control, and 44 ±3.2 units for the positive control.

Bottom panel: Distribution of rhodamine 123 fluorescence for cells grown in DMEM. Dotted line: negative control (no rhodamine). Solid line: positive control (40nM rhodamine 123, 30 minutes). The mean fluorescence is 2.8±0.1 units for the negative control, and 66±2.1 units for the positive control. The difference between the transmembrane potentials of cells grown in DMEM vs. cells grown in RPMI is significant ($p<0.005$, Student T- test)

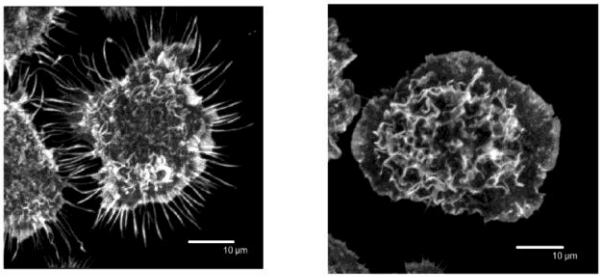

A B

Figure 5: changes in the cell morphology and actin cytoskeleton

Three dimensional reconstructions of the F-actin cytoskeleton (visualized by phalloidin staining) are shown, allowing visualization of the surface ruffles of the cells.
A: cell grown in RPMI1640 medium
B: cell grown in DMEM medium
The differences in shell shape and in membrane ruffles for cells grown in different media are obvious. Further details can be found in supplementary figures 2 and 3

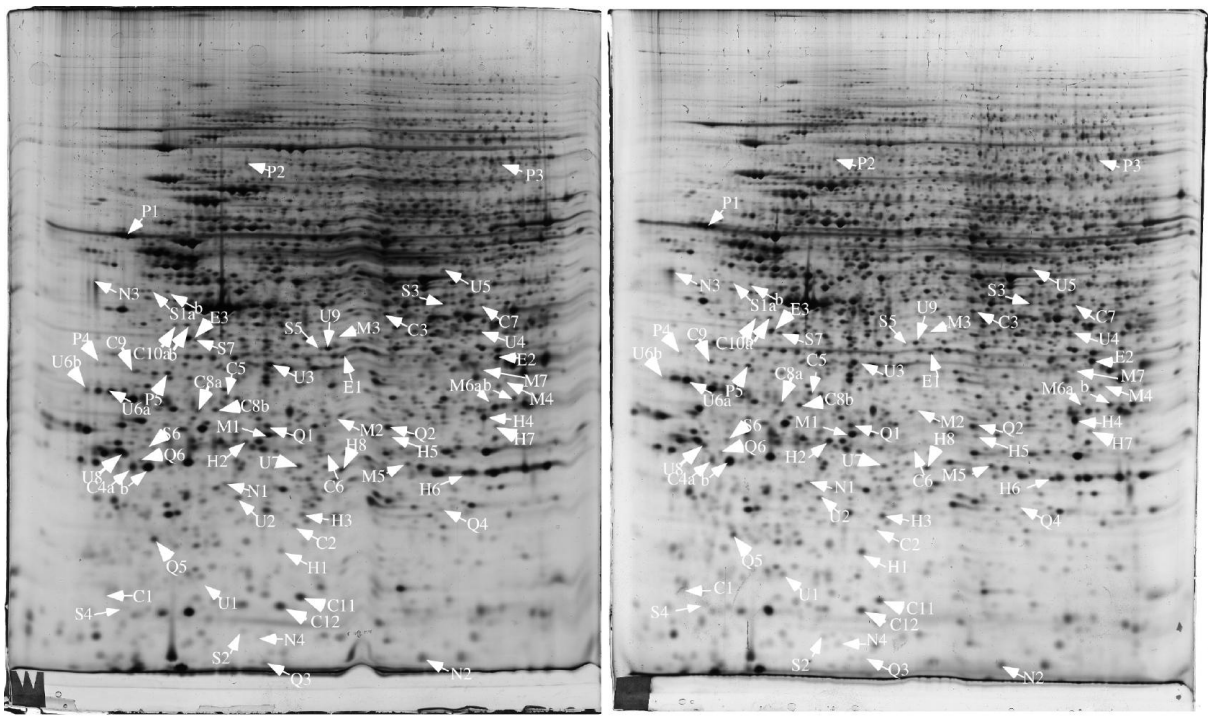

Figure 6: Proteomic analysis of total cell extracts by 2D electrophoresis: effect of copper oxide

Total cell extracts of J774A1 cells were separated by two-dimensional gel electrophoresis.
The first dimensions covered a 4-8 pH range and the second dimension a 15-200 kDa range.
Total cellular proteins (150 µg) were loaded on the first dimension gel.

A: gel obtained from control cells
B: gel obtained from cells treated with copper oxide (10 µg/ml, 24 hours)

The arrows point to spots that show reproducible and statistically significant changes between the control and nanoparticles-treated cells and to the control neighbor spots in some cases. Spot numbering according to Table 2